1-9-2006

The Starburst in the Abell 1835 Cluster Central Galaxy: A Case Study of Galaxy Formation Regulated by an Outburst from a Supermassive Black Hole

B. R. McNamara
Ohio University, USA

D. A. Rafferty
Ohio University, USA

L. Birzan
Ohio University, USA

J. Steiner
Ohio University, USA

M. W. Wise
Massachusetts Institute of Technology, USA

See next page for additional authors

The Astrophysical Journal, 648:164–175, 2006 September 1

THE STARBURST IN THE ABELL 1835 CLUSTER CENTRAL GALAXY: A CASE STUDY OF GALAXY FORMATION REGULATED BY AN OUTBURST FROM A SUPERMASSIVE BLACK HOLE

B. R. McNamara,[1] D. A. Rafferty,[1] L. Bîrzan,[1] J. Steiner,[1] M. W. Wise,[2] P. E. J Nulsen,[3]
C. L. Carilli,[4] R. Ryan,[1,5] and M. Sharma[1]
Received 2006 March 31; accepted 2006 May 10

ABSTRACT

We present an analysis of the starburst in the Abell 1835 cluster's cD galaxy. The dense gas surrounding the galaxy is radiating X-rays at a rate of $\sim 10^{45}$ ergs s^{-1}, which is consistent with a cooling rate of $\sim$1000–2000 $M_\odot$ yr^{-1}. However, *Chandra* and *XMM-Newton* observations found less than 200 $M_\odot$ yr^{-1} of cooling below $\sim$2 keV, a level that is consistent with the cD's current star formation rate of 100–180 $M_\odot$ yr^{-1}. One or more heating agents (feedback) must then be replenishing the remaining radiative losses. Supernova explosions and thermal conduction are unable to do so. However, the active galactic nucleus (AGN) is pumping $\simeq 1.4 \times 10^{45}$ ergs s^{-1} into the hot gas, which is enough power to offset most of the radiative cooling losses. The AGN jet power exceeds the radio synchrotron power by $\sim$4000 times, making this one of the most radiatively inefficient radio sources known. The jet power implies that the supermassive black hole has accreted at a mean rate of $\sim 0.3\ M_\odot$ yr^{-1} over the last 40 Myr or so, which is a small fraction of the Eddington accretion rate for a $\sim 10^9\ M_\odot$ black hole. The ratio of black hole growth rate by accretion to bulge growth by star formation is consistent with the slope of the (Magorrian) relationship between bulge and central black hole mass in nearby quiescent galaxies. The starburst follows the Schmidt-Kennicutt parameterizations, indicating that the local environment is not substantially altering the IMF and other conditions leading to the onset of star formation. The consistency between net cooling, heating (feedback), and the cooling sink (star formation) in this system resolves the primary objection to traditional cooling flow models.

Subject headings: cooling flows — galaxies: active — galaxies: clusters: general — galaxies: clusters: individual (Abell 1835) — galaxies: elliptical and lenticular, cD — galaxies: starburst — X-rays: galaxies: clusters

1. INTRODUCTION

The most luminous galaxies in the universe lie at the centers of galaxy clusters. Central dominant galaxies (which we refer to as cD galaxies) have masses of $\sim 10^{13}\ M_\odot$ and halos extending hundreds of kiloparsecs into the surrounding cluster (Sarazin 1986). They are able to grow to such large sizes by swallowing stars and gas from neighboring galaxies (Gallagher & Ostriker 1972; Hausman & Ostriker 1978; Merritt 1985) and by capturing the cooling intracluster gas (Fabian & Nulsen 1977; Cowie & Binney 1977). The bulges of many cD galaxies are currently growing rapidly through gas accretion and star formation, proceeding at rates of $\sim$10–100 $M_\odot$ yr^{-1} (Johnstone et al. 1987; McNamara & O'Connell 1989; 1993; Crawford et al. 1999; McNamara et al. 2004; Hicks & Mushotzky 2005; Rafferty et al. 2006; this paper). These rates rival or exceed those found in massive galaxies at redshifts in the range $z = 2$–3 (Juneau et al. 2005), yet they are found in nearby cooling flow clusters characterized by cuspy X-ray surface brightness profiles and rapidly cooling gas. The starbursts are fueled by $\sim 10^8$–$10^{11}\ M_\odot$ reservoirs of cold atomic and molecular gas (Jaffe et al. 2001, 2005; Donahue et al. 2000; Falcke et al. 1998; Heckman et al. 1989; Voit & Donahue 1997; McNamara et al. 1990; O'Dea et al. 1994; Taylor 1996; Jaffe 1990; Edge 2001; Salomé & Combes 2003). Bright optical emission nebulae and X-ray emission from clumps and filaments of gas at temperatures of $\sim 10^7$ K and densities of $\sim 10^{-2}$ cm^{-3} are a characteristic signature of these systems (McNamara et al. 2000, 2004; Fabian et al. 2003; Crawford et al. 2005; Jaffe et al. 2005). Under these conditions, the hot gas should cool and condense onto the central galaxy at rates of several hundred to over 1000 $M_\odot$ yr^{-1} (Fabian 1994). However, an inflow at this level would overwhelm these galaxies with cold gas and star formation exceeding the observed levels by factors of 10 or more. This implies that the cooling gas is deposited in an invisible form of matter or that it is condensing out of the intracluster medium at a much lower rate.

Progress on this problem stalled for more than a decade until the *Chandra* and *XMM-Newton* observatories revealed that most of the cooling gas is not condensing out of the hot intracluster medium, but rather it is maintained at X-ray temperatures by one or more heating agents. The spectra of cooling flows fail to show the soft X-ray emission lines emerging from gas cooling out of the X-ray band at the expected strength (Molendi & Pizzolato 2001; David et al. 2001; Fabian et al. 2001; Peterson et al. 2001, 2003; Tamura et al. 2001; Böhringer et al. 2002). Instead, the gas seems to be cooling down to about 1/3 of the average gas temperature at the expected rates, but most of it fails to continue to cool and condense onto the cD galaxy (Peterson et al. 2003). These observations do not, however, exclude cooling below X-ray temperatures at levels that are comparable to the observed star formation rates (McNamara 2004; McNamara et al. 2004; Hicks & Mushotzky 2005; Rafferty et al. 2006). Therefore, while the bulk of the cooling gas remains hot, enough may be condensing onto cD galaxies to drive star formation and to fuel the active galactic nucleus (AGN) at substantial rates.

[1] Astrophysical Institute and Department of Physics and Astronomy, Ohio University, Clippinger Labs, Athens, OH 45701.
[2] Kavli Institute, Massachusetts Institute of Technology, Cambridge, MA 02139-4307.
[3] Harvard-Smithsonian Center for Astrophysics, MS 70, 60 Garden Street, Cambridge, MA 02138; and University of Wollongong, Wollongong, NSW 2522, Australia.
[4] National Radio Astronomy Observatory, Socorro, NM 87801-0387.
[5] Department of Physics and Astronomy, Arizona State University, Tempe, AZ 85287-1504.

Potential heating mechanisms include thermal conduction from the hot gas surrounding the cool core (Tucker & Rosner 1983; Bertschinger & Meiksin 1986; Narayan & Medvedev 2001), subcluster mergers (Gómez et al. 2002), supernovae (Silk et al. 1986), and AGN outbursts (Tabor & Binney 1993; Binney 2004; Soker et al. 2001; Ciotti & Ostriker 1997), among others. However, the stringent demands on these mechanisms have been met with varying degrees of success. X-ray cooling is persistent, powerful, and widespread. An effective heating mechanism must be able to cope by producing a heat flux of $\sim 10^{44}$–10^{45} ergs s^{-1} persisting over several billion years and distributing the heat throughout a cooling volume that is comparable to the full extent of the central galaxy. Supernova explosions are generally too weak and too localized; mergers are powerful enough but cannot be relied on to provide a persistent source of heat; and conduction proceeds with great difficulty deep in the cool cores of clusters. Recurrent AGN outbursts have emerged as the agent best able to meet these requirements, although thermal conduction still may play a significant role near the cooling radius (e.g., Ruszkowski & Begelman 2002; Rosner & Tucker 1989; Narayan & Medvedev 2001; Voigt et al. 2002; Soker et al. 2002; Zakamska & Narayan 2003).

The cD galaxies are known to harbor powerful radio sources (Burns 1990). Outbursts from AGNs associated with these sources generate cavities, ripples, and shock fronts in the hot gas surrounding them, and the energy dissipated is enough to balance radiative cooling losses in many systems (McNamara et al. 2000, 2001, 2005; Bîrzan et al. 2004; Young et al. 2002; Forman et al. 2005; Nulsen et al. 2002, 2005a, 2005b; Blanton et al. 2003; Heinz et al. 2002; Kraft et al. 2006; Rafferty et al. 2006; and others). These outbursts generate $\sim 10^{55}$ ergs in giant elliptical galaxies and groups (Finoguenov & Jones 2001), to upward of $\sim 10^{61}$ ergs in rich clusters (Bîrzan et al. 2004; McNamara et al. 2005; Nulsen et al. 2005a, 2005b). This is enough energy to quench cooling entirely in isolated elliptical galaxies (Finoguenov & Jones 2001; Best et al. 2006), and to drive outflows and buoyant bubbles that regulate cooling flows (Rafferty et al. 2006). The most powerful outbursts are able to heat the gas beyond the cooling region (McNamara et al. 2005; Nulsen et al. 2005a, 2005b) and contribute to the overall entropy excess in clusters (Voit & Donahue 2005). The past few years have seen remarkable growth in the number of computer simulations of pressure-confined jets pushing through hot atmospheres. The simulations generally show that much of the jet energy is thermalized and thus is able to heat the gas. However, the important details concerning how and how much of the jet energy is thermalized and distributed throughout the cooling region, and how the cavities are stabilized are not entirely understood (e.g., Reynolds et al. 2002; Basson & Alexander 2003, Kaiser & Binney 2003; Brüggen & Kaiser 2001, 2002; Brüggen 2003; Soker et al. 2001; Brighenti & Mathews 2002; Churazov et al. 2001, 2002; Quilis et al. 2001; De Young 2003; Jones & De Young 2005; Omma et al. 2004; Ruszkowski et al. 2004; Vernaleo & Reynolds 2005; Piffaretti & Kaastra 2006; and many others).

These issues are deeply rooted in the more general problem of galaxy formation. In the standard cold dark matter (CDM) hierarchy (White & Rees 1978), small halos merge into larger ones; while the captured baryons cool and condense onto the progenitors of mature galaxies, a process that should still be occurring in clusters today (Cole 1991; Blanchard et al. 1992; Sijacki & Springel 2006). This paradigm successfully describes the distribution of matter on large scales. However, it has difficulty dealing with the fact that even the biggest galaxies seemed to have formed quickly. Furthermore, CDM models that include gravity alone overpredict the fraction of cold baryons (Balogh et al. 2001), and thus, they predict bigger galaxies and more of them than are observed (Voit 2005). The jumbo cD galaxies are a case in point. Although they have grown to enormous sizes, they should have absorbed more of the cooling baryons in clusters and grown larger still (Sijacki & Springel 2006). Instead of condensing onto the cD, most of the baryons in clusters reside today in the hot gas between the galaxies. The work-around involves nongravitational heating by early supernova explosions and AGNs. Supernova explosions are surely important at some level, and they are essential for enriching the gas with metals (Metzler & Evrard 1994; Borgani et al. 2002; Voit 2005). However, they are generally too feeble and localized to truncate star formation in massive galaxies (Borgani et al. 2002). Furthermore, in the closely related "preheating" problem, they have difficulty boosting the entropy level of the hot gas to the observed levels, particularly in cooler clusters (Wu et al. 2000; Voit & Donahue 2005; Donahue et al. 2005).

A great deal of progress on these problems has been made in recent work showing that powerful AGN outbursts in cD galaxies can supply enough energy to reduce or quench cooling flows and thus regulate the growth of massive galaxies (e.g., Bîrzan et al. 2004 and references therein). At the same time, lower limits on the outburst energies, which can now be measured reliably using X-ray-cavity and shock properties, imply that the supermassive black holes powering them are growing at typical rates of $\sim 10^{-3}\, M_\odot\ \mathrm{yr}^{-1}$ (Rafferty et al. 2006). In some cases the growth rates are approaching or modestly exceed $\sim 1\, M_\odot\ \mathrm{yr}^{-1}$ (McNamara et al. 2005; Nulsen et al. 2005a, 2005b), rivaling those during the most rapid periods of black hole growth in the early universe. Except in the most powerful outbursts, they accrete at a small fraction of the Eddington rate (Rafferty et al. 2006) through a combination of cold disk accretion and Bondi-Hoyle accretion of the hot gas surrounding them (Rafferty et al. 2006). Bondi-Hoyle accretion is not required, as there is an adequate supply of cold fuel in cD galaxies to accommodate extended periods of rapid accretion.

Supermassive black holes may reside at the centers of most if not all massive bulges, and thus they appear to be an inevitable consequence of galaxy formation (Kormendy & Richstone 1995). The well-known correlations between bulge luminosity, velocity dispersion, and central black hole mass (Gebhardt et al. 2000; Ferrarese & Merritt 2000) show that the growth of galaxies and supermassive black holes are closely connected, perhaps in part through the regulation of inflowing gas by AGN outbursts (Begelman & Nath 2005; Springel et al. 2005). Cooling flows have emerged among the few places in the nearby universe where bulge and supermassive black hole growth in massive galaxies can be examined in quantitative detail. The conditions there serve as a test bed for feedback-driven galaxy formation and nongravitational heating models (Sijacki & Springel 2006).

We examine these issues using deep *U*- and *R*-band images of the central region of the $z = 0.252$ cluster Abell 1835, we compare them to new and archival *Chandra* images, and we examine the relationships between cooling and star formation in the cD galaxy. Throughout this paper, we assume $H_0 = 70$ km s^{-1} Mpc^{-1}, $\Omega_m = 0.3$, $\Omega_\Lambda = 0.7$, $z = 0.2523$, a luminosity distance of 1274 Mpc, and a conversion between angular and linear distance of 3.93 kpc arcsec^{-1}.

2. X-RAY AND OPTICAL OBSERVATIONS

2.1. *Optical Observations*

The optical observations were obtained with the Kitt Peak National Observatory's 4 m telescope equipped with the T2KB

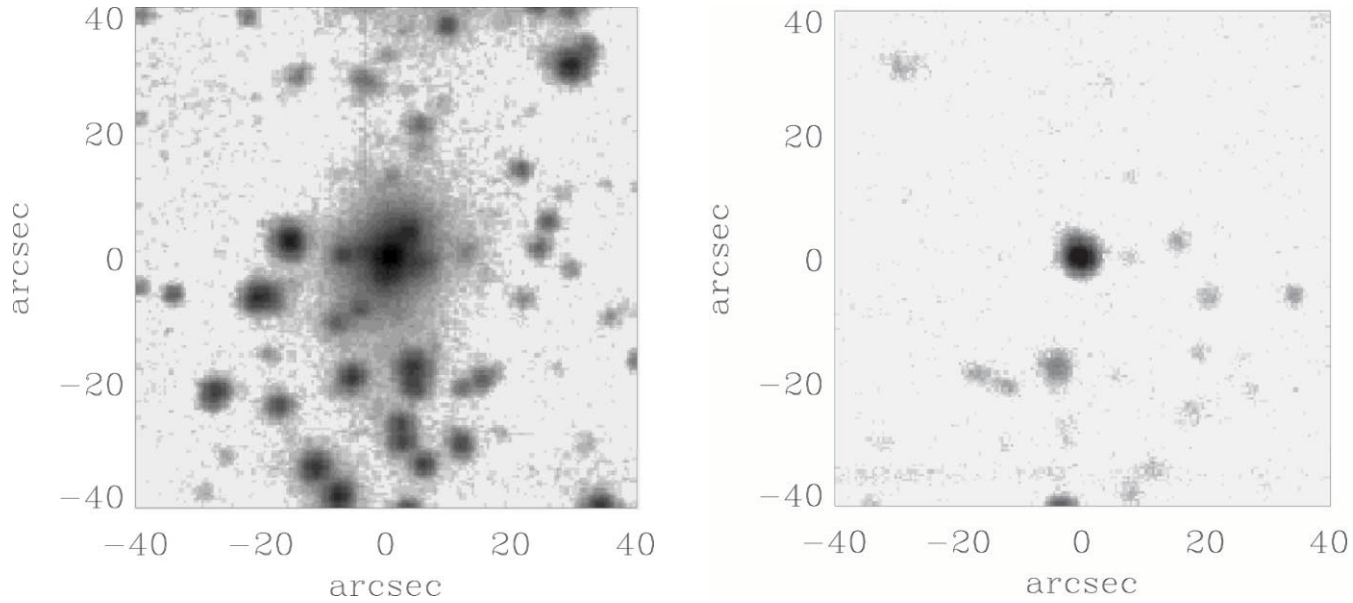

FIG. 1.—*Left*: *R*-band image of the $40'' \times 40''$ (157 kpc × 157 kpc) region of the cluster centered on the cD galaxy. *Right*: *U*-band image of the same region, but with the background population of the cD removed, showing the central starburst.

CCD camera at prime focus in 1995 February. This configuration delivered a plate scale of $0\farcs47$ pixel^{-1}. Images were exposed through the standard *U*-band plus liquid copper sulfate red-leak-blocking filter and an *R*-band filter with an effective wavelength of 7431 Å that avoids contamination from strong emission lines. Exposure times were 2100 s in *U* and 1200 s in *R*. The target images were taken in short-scan mode, which shifts charge in the CCD during an exposure to improve the flat-field quality of the images. The target images were individually flat-fielded using twilight sky images; the bias level was subtracted from each image, and they were then combined into the science images used in our analysis. The seeing throughout the observations was $\simeq 2''$–$3''$. The sky was transparent, and several photometric standard stars were observed throughout the evening.

2.2. *Structure of the Central Galaxy*

The *R*-band image of the central $40'' \times 40''$ (157 kpc × 157 kpc) of the cluster is shown in the left panel of Figure 1. The light is dominated by the central cluster cD galaxy located at R.A. = $14^{\rm h}01^{\rm m}02\fs01$, decl. = $+02^\circ52'41\farcs7$ (J2000.0), and nearly two dozen fainter galaxies, several of which are projected onto the cD's envelope. The right panel of Figure 1 shows the *U*-band image after subtracting a model of the background galaxy leaving only the blue starburst region at the center. The starburst is concentrated within a $9''$ (35 kpc) radius of the nucleus. It is roughly circular in projection with no obvious resolved substructure or tidal features. The starburst is discussed further in § 3.

The *U*- and *R*-band surface brightness profiles are presented in Figure 2. The profiles were constructed using elliptical annuli with fixed ellipticities of 0.22 and position angles of $\simeq 331^\circ$, chosen by fitting the mean values of the *R*-band isophotes beyond the starburst region. The surrounding galaxies were removed from the images in order to avoid contaminating the light of the cD. The surface brightness profiles in each band were flux calibrated using Landolt standards and transformed to the rest frame using *K*-corrections from Coleman et al. (1980). The *K*-corrections in *U* and *R* are 1.176 mag and 0.258 mag, respectively. Fluxes were corrected for Galactic foreground extinction using the prescriptions of Cardelli et al. (1989), assuming a foreground color excess of $E(B-V) = 0.03$. The profiles include statistical error bars (imperceptible in all but the outer points), and systematic error confidence intervals (*dashed lines*) determined using the methods described in McNamara & O'Connell (1992).

The halo light beyond the starburst declines according to an $R^{1/4}$ profile. It rises above the extrapolation of the $R^{1/4}$ beyond $16''$ (63 kpc), where the characteristic cD halo becomes visible (Schombert 1986). Apart from the blue core, these properties are normal for central cluster galaxies within a redshift $z \lesssim 0.1$ (Porter et al. 1991).

In Figure 3 we show the $(U-R)_{K,0}$ color profile derived from the surface brightness profiles. To establish a point of reference, the normal rest-frame colors for a cD galaxy generally lie within the range of 2.3–2.6 in the inner few tens of kiloparsecs,

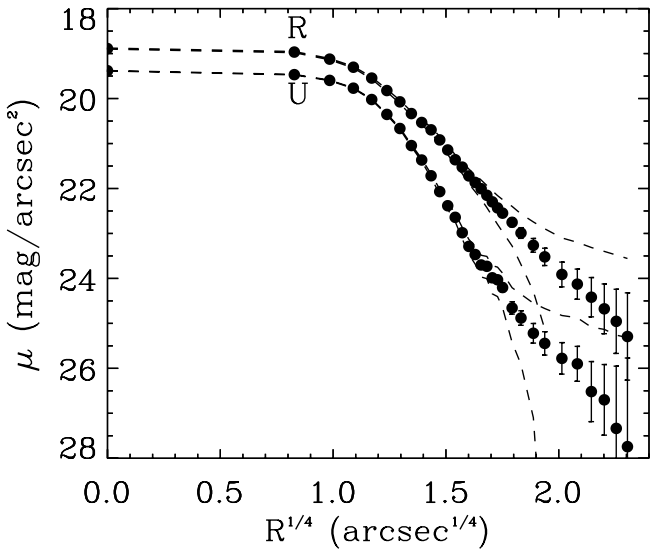

FIG. 2.—The *U*-band and *R*-band surface brightness profiles of the cD galaxy. The dashed lines represent the systematic uncertainty associated with sky background subtraction

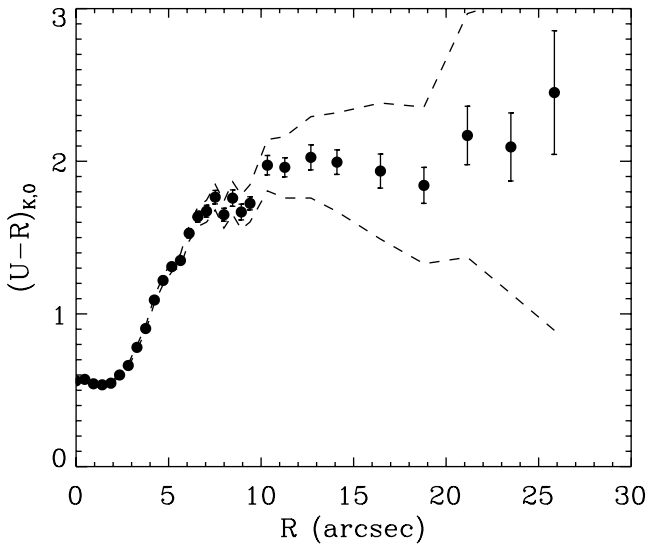

FIG. 3.—The $U - R$ color profile of the cD galaxy showing the central blue colors associated with the starburst. Normal colors are ~2.3–2.6. The dashed lines represent the systematic uncertainty associated with sky background subtraction

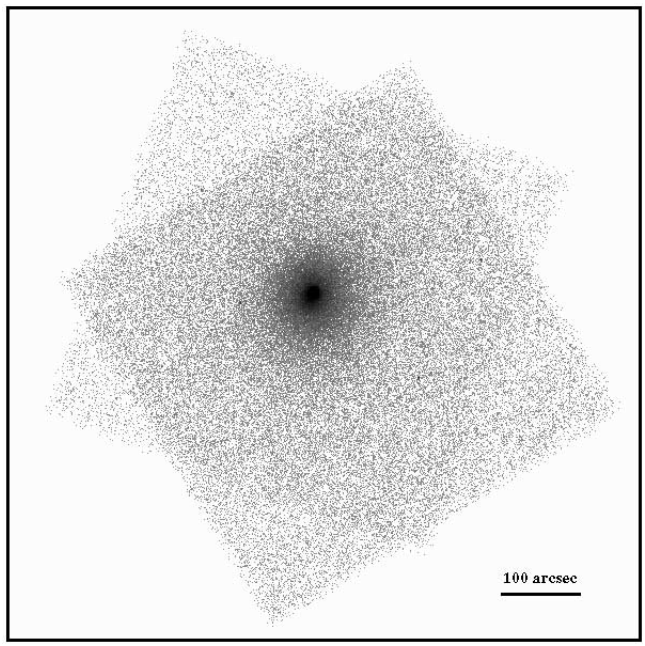

FIG. 4.—X-ray image of the cluster made with the combined 30 ks exposure.

while the nuclear colors tend toward the red end of this range (Peletier et al. 1990). Figure 3 shows that the cD galaxy's $U - R$ color is anomalously blue in the inner 9″ or so. It's central color is approximately 1.3 mag bluer than the halo color of $(U - R)_{K,0} \sim 2$ between 12″ and 17″ or so (47–67 kpc). The colors redden to a relatively normal color of $(U - R)_{K,0} \sim 2.3$ in the halo and envelope beyond 17″. This profile is the characteristic signature of a starburst, which we discuss in detail in § 3.

2.3. *Chandra X-Ray Observations*

The cluster was observed three times by *Chandra*: on 1999 December 11 for 19.5 ks (ObsID 495), on 2000 April 29 for 10.7 ks (ObsID 496), and again in 2005 December for 66.5 ks. The 66.5 ks exposure, which we discuss in § 4.3, is the first part of a longer, 250 ks ACIS-I observation being made in pursuit of a separate project. The 1999 and 2000 images were made with the back-illuminated ACIS-S3 CCD. We analyzed this data using the Chandra Interactive Analysis of Observations (CIAO) 3.2.3 with the calibrations of CALDB 3.1.0. The level 1 event files were reprocessed to apply the latest gain and charge-transfer-inefficiency correction and filtered for bad grades. The light curves of the resulting level 2 event files showed no strong flares in either observation. However, comparisons with *XMM-Newton* observations of Abell 1835 (Majerowicz et al. 2002; Jia et al. 2004) show that observation 495 was affected by a mild flare (see Markevitch 2002). This flare has the effect of significantly raising the modeled temperatures in the outer parts of the cluster (Schmidt et al. 2001). We have therefore used only observation 496 for spectral analysis. However, since the flare is likely to be spatially uniform, we used both observations, appropriately corrected for exposure, for the imaging analysis.

The image of the combined 30 ks equivalent exposure is shown in Figure 4. Outside of the core, the X-ray emission is fairly smooth and symmetrical in an elliptical distribution with an ellipticity of ~0.12 and position angle of ~340°. Inside the core, however, the emission is more complex, with twin, off-center peaks and two surface brightness depressions on either side of the cD galaxy's nucleus (see § 4.3).

To find the radial gas density and temperature distributions, we extracted spectra from observation 496 with at least 3000 counts in each concentric annulus about the X-ray centroid with the ellipticity and position angle given above. The appropriate blank-sky background file, normalized so that the count rate of the source and background images match in the 10–12 keV band, was used for background subtraction.

In the following spectral analyses, all spectra were analyzed between the energies of 0.5 and 7.0 keV using XSPEC 11.3.2 (Arnaud 1996), and the spectra were binned with a minimum of 30 counts. To obtain temperatures and abundances, we used a model of a single-temperature plasma (MEKAL) plus the effects of Galactic absorption (WABS). Abell 1835 is located along the same line of sight as the Galactic North Polar Spur (Majerowicz et al. 2002), resulting in excess background at low energies. However, we are interested only in the bright inner parts of the cluster where the spur's contribution to the background has a negligible effect on our fits. The redshift was fixed at $z = 0.253$, and the absorbing column density was fixed at the Galactic value of $N_{\rm H} = 2.3 \times 10^{20}$ cm^{-2} (Dickey & Lockman 1990). The temperature, abundance, and model normalization were allowed to vary. To investigate the effects of projection and to derive electron densities (n_e), we deprojected the spectra by including the PROJCT model in XSPEC with the single-temperature model (PROJCT × WABS × MEKAL) and by fitting all spectra simultaneously. We used the deprojected temperature and density ($n = 2n_e$) to determine the pressure ($P = nkT$), entropy ($S = kT/n^{2/3}$), and cooling time (Böhringer & Hensler 1989) of the gas in each annulus.

The profiles, shown in Figures 5–8 are in overall agreement with the analyses of the same data by Markevitch (2002) and Schmidt et al. (2001) and with the analyses of *XMM-Newton* data (e.g., Majerowicz et al. 2002; Jia et al. 2004). The temperature of the gas rises from ~4 keV in the center to ~11 keV at a distance of ~2′. As expected, the temperatures obtained from deprojection are slightly lower in the central regions than the projected temperatures, as the projected temperatures include emission from the hot outer parts of the cluster that is accounted for in deprojection. The abundance profile shows an increase toward the center, rising from approximately 1/3 of the solar abundance at a distance of ~2′ to roughly solar abundance at the

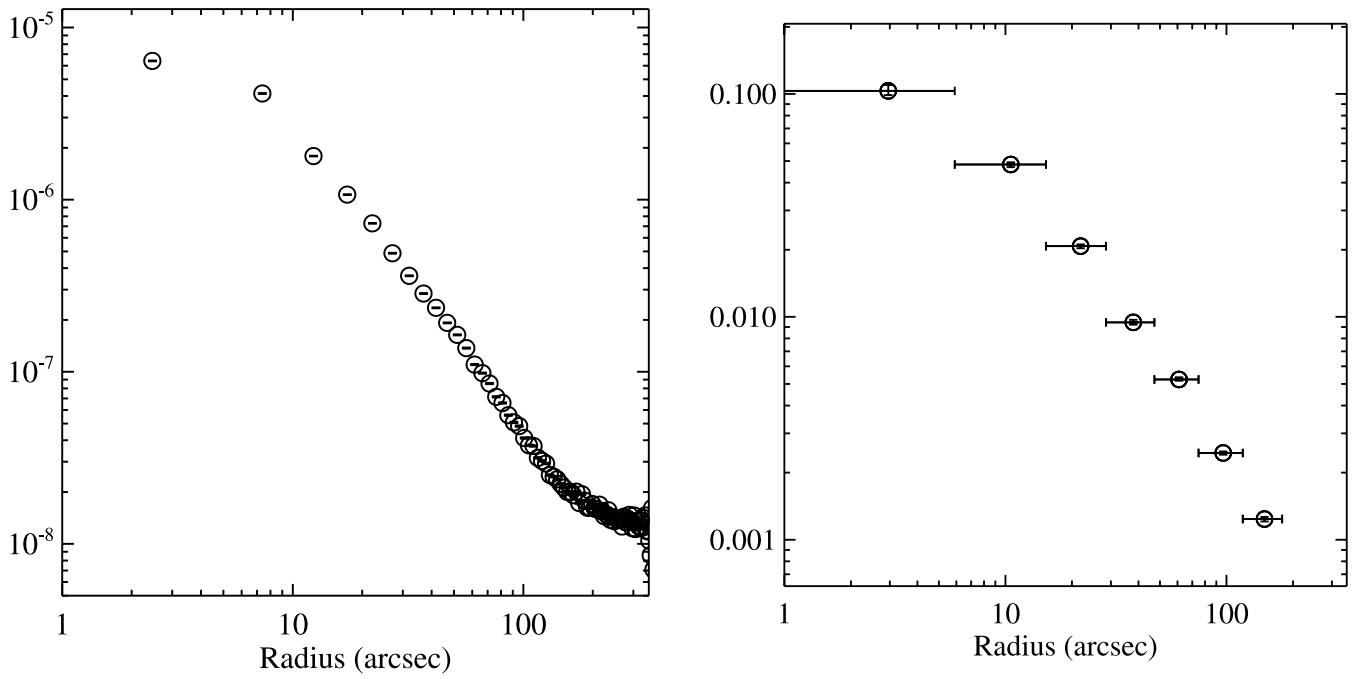

FIG. 5.—*Left*: X-ray surface brightness profile. *Right*: Density profile of the hot gas.

center. A spectrum extracted for the entire cluster within a radius of 3′ gives an average, emission-weighted temperature of $kT = 7.8 \pm 0.3$ keV and abundance of $Z = 0.39 \pm 0.05\ Z_{\odot}$.

The cooling rate of the gas was estimated by adding a cooling flow model (MKCFLOW) to the single-temperature model [i.e., WABS × (MEKAL + MKCFLOW)] and fitting it to spectra extracted from the cooling region ($r_{\rm cool} = 41''$), defined to be the region inside which the cooling time is $<7.7 \times 10^9$ yr. Fits were made to both a single spectrum of the entire cooling region and to spectra extracted in concentric, deprojected elliptical annuli. In the latter case, to force all cooling to be within the cooling region, the MKCFLOW model normalization was set to zero outside the cooling region. For each spectrum, the temperature of the MEKAL component was tied to the high temperature of the MKCFLOW component, and the MEKAL and MKCFLOW abundances were tied together. Parameters were fixed or free to vary as described above.

We investigated several different cooling models. One explored the maximum cooling rate below the X-ray band allowed by the data. This model was constructed by fixing the low temperature of the cooling flow model to 0.1 keV. Another explored the maximum rate of cooling from roughly the mean gas temperature to the

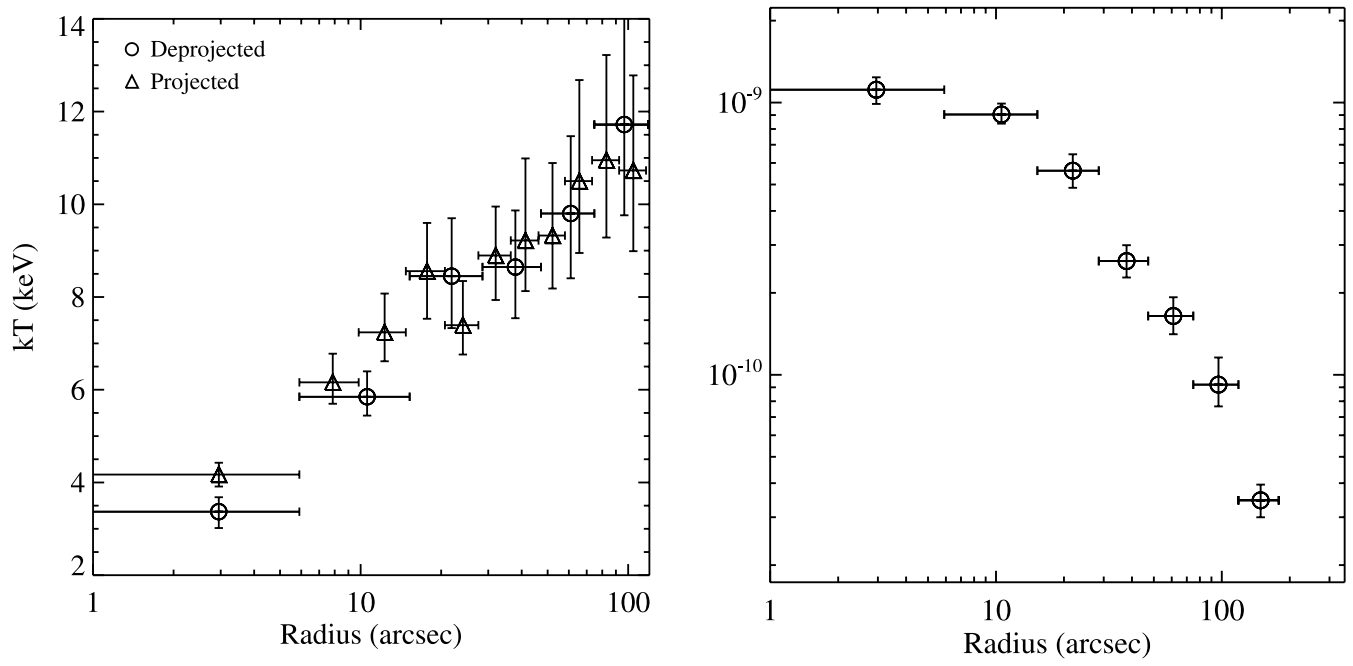

FIG. 6.—*Left*: Projected (*triangles*) and deprojected (*circles*) X-ray temperature profile of the hot gas. *Right*: Central pressure profile of the hot gas.

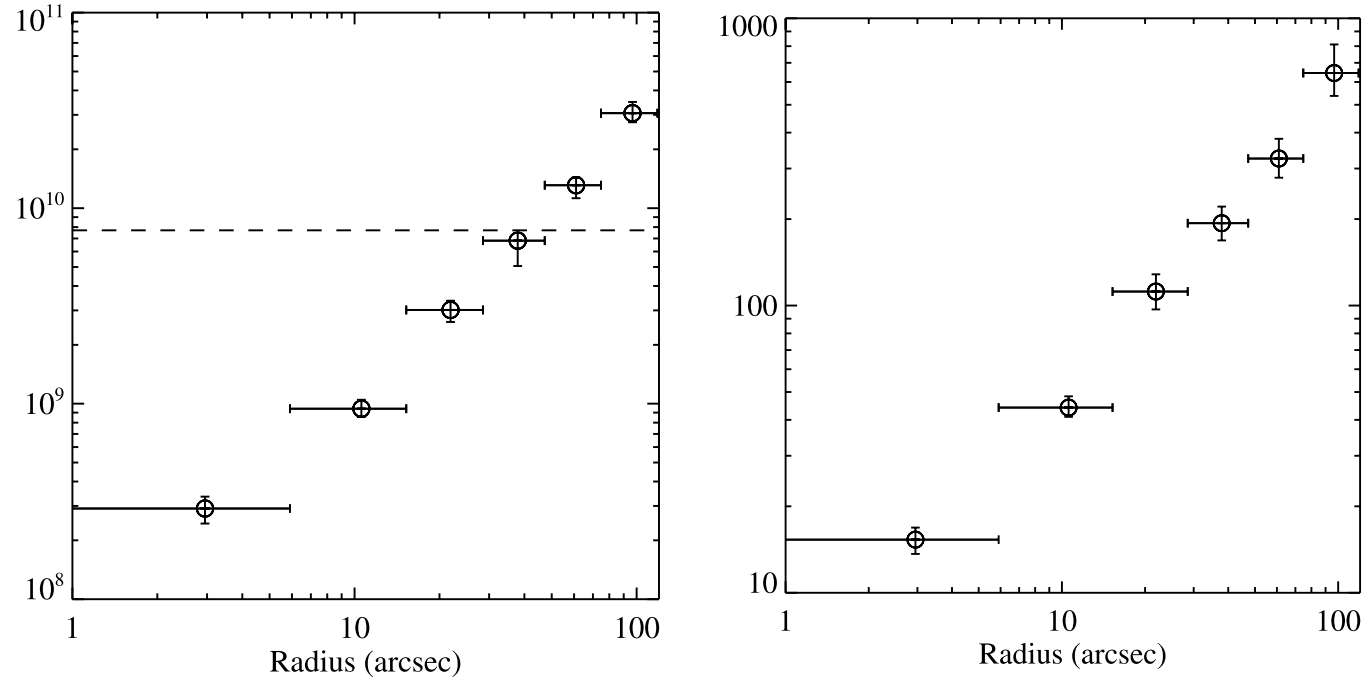

FIG. 7.—*Left*: Cooling time profile for the hot gas. The dashed line represents a cooling time of 7.7×10^9 yr, which is the look-back time to a redshift of 1, which we assume to be roughly the epoch of cluster formation. This corresponds to a cooling radius of 41″, or 161 kpc *Right*: Entropy profile of the hot gas.

lowest detected temperature within the X-ray band by allowing the low temperature to vary. The first model found cooling limits as low as $\sim 30\ M_\odot\ \mathrm{yr}^{-1}$, while the second model allowed for cooling at rates of several thousand solar masses per year. We also attempted to reproduce the cooling profile of Schmidt et al. (2001) using newer calibration files, but were unable to do so. Because of the low exposure level and high particle background, it was difficult to find a stable and robust solution to the cooling models. We arrived at the conclusion that Peterson et al.'s (2003) upper limit of $<200\ M_\odot\ \mathrm{yr}^{-1}$ is the most reliable measurement available, and we have adopted this value throughout the paper.

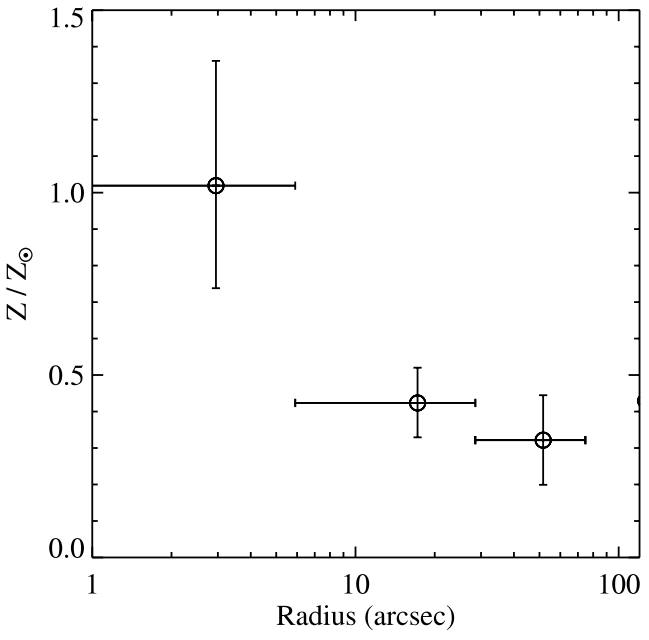

FIG. 8.—Abundance profile of the hot gas in solar units.

3. THE STARBURST IN ABELL 1835

3.1. *Star Formation Rates from Near-Ultraviolet Imaging*

Except where otherwise noted, our approach, methods, and rationale closely follow the discussion of the starburst in Abell 1068 (McNamara et al. 2004). Briefly, we estimate the luminosity, mass, and age of the starburst, first by measuring the light emerging from the starburst population alone in the *U* and *R* bands. This involves modeling the light profile of the older background stellar population in each band and subtracting it from the respective image. The profiles generally follow an $R^{1/4}$ law beyond the starburst, but the profiles soften considerably in the center of the galaxy, where the true shape of the background light is poorly known. We have therefore taken two approaches that effectively give lower and upper bounds to the starburst population's flux and color. The first involves an extrapolation of a spline fit to the halo profile into the core of the galaxy running underneath the starburst light (see McNamara et al. 2004 and references therein). Second, we scaled the *R*-band profile, which is minimally affected by the burst, to fit the *U*-band light profile underneath the burst. Both models were subtracted from the images leaving the starburst in residual.

The ratios of the residual and model light give the fraction of light, $f(\lambda)$, contributed by the starburst population in each band. These methods give *U*-band light fractions of 25% and 50%, respectively, within 9″ of the nucleus. Since the real fraction depends on the true shape of the underlying light profile, we treat these values as lower and upper limits. In contrast, the starburst contributes only a few percent of the light in the *R* band. The starburst population mass is then found as $M_* = M/L(U)_* f(U) L(U)$, where $M/L(U)_*$ is the model-dependent *U*-band mass-to-light ratio of the starburst population and $L(U)$ is its total *U*-band luminosity.

The starburst's age is estimated by comparing its color to two simple but representative stellar population histories based on the Bruzual & Charlot (2003) population models: an instantaneous

burst and continuous star formation, each of which assumes a Salpeter initial mass function (IMF) and solar abundances (the choice of abundance has little effect on our results). We found the *U*-band luminosity of the starburst population alone to be $L(U)_* \equiv f(U)L(U) = (2.6\text{–}5.9) \times 10^{11}\ L_\odot$, before correcting for internal extinction. The intrinsic color of the starburst population provides a constraint on the population's age, history, and mass-to-light ratio (see McNamara et al. 2004). We find a probable range for the starburst population's color of $(U - R)_* \sim -0.3$ to the bluest color that is theoretically possible $(U - R)_* \sim -1.4$.

The blue end of the color range is broadly consistent with an instantaneous burst that occurred less than 3 Myr ago involving a starburst population mass of between 9×10^9 and $2 \times 10^{10}\ M_\odot$. The red end of the color range is consistent with an aging, instantaneous burst that occurred 32 Myr ago or ongoing (continuous) star formation for 320 Myr. The instantaneous and continuous starburst population masses are $2 \times 10^{10}\ M_\odot$ and $3 \times 10^{10}\ M_\odot$, respectively. The star formation rate for continuous star formation over the past 320 Myr is $100\ M_\odot\ \mathrm{yr}^{-1}$. This is consistent with the spectroscopic rate found by Crawford et al. (1999), but somewhat lower than Allen's (1995) rate.

The data are inconsistent with star formation that has been ongoing for $\gtrsim$1 Gyr, as might be expected in a long-lived cooling flow (Fabian 1994), but the measurement uncertainties are too large to consider more complex star formation histories. The instantaneous burst model is always an unrealistic approximation. However, using colors alone we cannot rule out an intense, short-lived burst of star formation fueled by a rapid infusion of gas supplied, perhaps, by a merger. Nevertheless, the enormous amount of molecular fuel ($\sim 10^{11}\ M_\odot$) that must be consumed by the starburst, even at the highest rates, suggests we are dealing with a longer term event that is better described by continuous star formation extending over several hundred million years.

The *U*-band luminosities, masses, and star formation rates above have not been corrected for internal extinction. Doing so reliably requires high-resolution images in two or more bands, which we do not have. Although no dust lanes are seen in our images, Crawford et al. (1999) estimated internal extinction at the level of $E(B - V) = 0.38$, based on anomalous Balmer emission-line ratios. Correcting this effect would increase the luminosity masses and the star formation rate above by a factor of about 1.8, giving a corrected star formation rate of $180\ M_\odot\ \mathrm{yr}^{-1}$. The reddening would also affect the population colors, possibly leading to a somewhat younger age, which would lessen the accreted mass somewhat. A star formation rate between 100 and $180\ M_\odot\ \mathrm{yr}^{-1}$ is broadly consistent with our data.

3.2. *Far-Ultraviolet, Infrared, and* Hα*-based Star Formation Rates*

Other evidence for an ongoing starburst include the detections of $9 \times 10^{10}\ M_\odot$ of molecular gas (Edge 2001) and a far-infrared 60 μm flux of 330 ± 69 mJy (emission at 100 μm is absent from the *IRAS* addscans). The corresponding far-infrared luminosity of $L_{\mathrm{FIR}}(60\ \mu\mathrm{m}) = 3 \times 10^{45}$ ergs s^{-1}, or $\sim 10^{12}\ L_\odot$, places Abell 1835 nearly in the class of ultraluminous infrared galaxies.

Assuming that the far-infrared and nebular emission are powered by star formation, they provide independent estimates of the star formation rate. Folding the infrared luminosity through Kennicutt's (1998) relation, we find a star formation rate of $138\ M_\odot\ \mathrm{yr}^{-1}$, a value that lies midway between the dust and dust-free *U*-band estimates.

Kennicutt's relationship between Hα luminosity and star formation rate gives a poorer match. Using the Crawford et al. (1999) Hα luminosity 5.12×10^{42} ergs s^{-1}, after correcting for internal extinction and different cosmologies, we arrive at a star formation rate of only $41\ M_\odot\ \mathrm{yr}^{-1}$. This is substantially lower than the *U*-band and infrared continuum estimates. However the Hα luminosity is an indirect and hence less reliable star formation indicator than the ultraviolet continuum.

Using the far-ultraviolet imager on the *XMM-Newton* observatory, Hicks & Mushotzky (2005) found a star formation rate of $123\ M_\odot\ \mathrm{yr}^{-1}$, which is consistent with our rate. As we do, they assumed a Salpeter IMF. However, lacking color information, they adopted a 900 Myr age for the population, which is 3 times the age implied by the starburst population's color. An age of 900 Myr implies a color of $(U - R) \sim 0$, which is three-tenths of a magnitude redder than our measurement, but it lies at the limit of the uncertainty. If we adopt for the moment a 900 Myr old population with a corresponding *U*-band mass-to-light ratio of $\sim$0.18, we arrive at a star formation rate of $50\ M_\odot\ \mathrm{yr}^{-1}$. This rate is comparable to the Hα rate, but it lies far below the infrared and nominal *U*-band rates. We regard this as a tight lower limit to the star formation rate in Abell 1835.

3.3. *Abell 1835 and the Schmidt-Kennicutt Law for Star Formation*

Using a large sample of disk galaxies and infrared-selected starburst galaxies, Kennicutt (1998) found a series of relationships between the surface densities of both molecular gas and star formation and the typical orbital periods of particles within the starburst regions. Normal disk galaxies, the centers of normal disks, and starburst galaxies spanning a broad range of gas and stellar surface densities lie along a series of relatively tight power-law relationships resembling the classical Schmidt (1959) law. This level of continuity suggests that the gross properties of star formation, such as the IMF, are not strongly effected by local environmental conditions.

It would therefore be worthwhile to compare cooling flow starbursts lying in high-pressure cluster cores with and without strongly interacting AGNs to see if they follow global trends. We include in this comparison the cD galaxy in Abell 1068, which like Abell 1835, harbors a massive starburst (McNamara et al. 2004), but unlike Abell 1835, is apparently not currently experiencing an energetic AGN outburst. We measured the surface densities of star formation and molecular gas in both systems, and we calculated the orbital period at the edge of the star formation regions following Kennicutt's (1998) prescription. Our results are listed in Table 1.

The values in Table 1 follow Kennicutt's (1998) relationship between star formation rate density versus gas surface density $\Sigma_{\mathrm{SFR}} \propto \Sigma_{\mathrm{gas}}^{1.4}$ for starburst galaxies, normal disk galaxies, and the centers of normal disks. However, they are not located among the infrared starburst galaxies, as one might expect. Instead, they lie among the centers of normal disk galaxies. This is primarily due to the large spatial extent of the molecular gas (Edge & Frayer 2003) and star formation regions, which results in lower surface densities than the infrared starbursts in Kennicutt's sample. This is true even though the cooling flow star formation rates dwarf those of spiral galaxies. At the same time, the orbital periods of stars at the edges of the cooling flow star formation regions are between 200 and 600 Myr, which is substantially longer than Kennicutt's more compact starbursts. This implies that star formation is consuming the molecular gas before it has had time to execute more than a few orbits, which is again consistent with Kennicutt's parameterizations and assumptions now routinely adopted in semi-analytical models of galaxy formation (e.g., Kauffman 1996; Croton et al. 2006).

TABLE 1
STARBURST PROPERTIES

Cluster	SFR ($M_\odot$ yr^{-1})	M_{gas} ($M_\odot$)	R_{burst} (kpc)	$\log \Sigma_{SFR}$ ($M_\odot$ yr^{-1} kpc^{-2})	$\log \Sigma_{gas}$ ($M_\odot$ pc^{-2})	τ^a_{dyn} (yr)	$\log \Sigma_{gas}/\tau_{dyn}$ ($M_\odot$ yr^{-1} pc^{-2})
Abell 1835	100−180	9×10^{10}	30	−1.19	1.51	6.6×10^8	2.14[a]
Abell 1068	20−70	4×10^{10}	10	−0.65	2.12	2.2×10^8	2.25[a]

[a] Assumes a stellar velocity dispersion of 281 km s^{-1} (Bîrzan et al. 2004).

The molecular gas almost certainly originated outside of the cD galaxy. Whether it was stripped from a passing galaxy or whether it condensed out of the cooling flow is unknown. In the context of the cooling flow, its mass corresponds to approximately 4.5×10^8 yr of accumulated gas from a 200 $M_\odot$ yr^{-1} flow. This timescale is close to both the cooling and orbital timescales within the starburst. The gas may have pooled following an interruption in a time-dependent cooling flow, as might be expected in AGN-regulated systems. Alternatively, it may be that the molecular gas accumulated at the center of the galaxy until it reached a critical density for the onset and maintenance of star formation. If so, the apparent agreement between the cooling and star formation rates implies that the cooling gas is feeding the reservoir of molecular gas now at about the mean rate it has done so for the past several hundred million years.

It is worth noting that earlier suggestions that the high ambient pressure in cooling flows might alter the Jean's unstable molecular cloud mass leading to an anomalous IMF (e.g., Sarazin & O'Connell 1983) are not supported by this analysis. Furthermore, with growing evidence for feedback-driven quenching of cooling flows, it is no longer necessary to appeal to a faint stellar repository that would justify the need for an anomalous IMF.

3.4. *Chemical Enrichment from the Starburst*

Metal enrichment by a starburst of this size is significant enough to enhance the metallicity of the gas in the core. Figure 8 shows the metal abundance rising from roughly 1/3 of the solar abundance at 200 kpc to nearly solar metallicity in the starburst region. A similar rise but with a somewhat smaller amplitude (and poorer spatial resolution) was also seen in an *XMM-Newton* analysis of Abell 1835 by Majerowicz et al. (2002). Their *XMM* observation follows the metallicity profile out to about 800 kpc, where the cluster's average metallicity is about 1/4 of the solar value. The metallicity begins to rise at a radius of about 160 kpc (50″), which is beyond the edge of our profile in Figure 8. Following the procedure of Wise et al. (2004), we find that the starburst alone is capable of enriching the gas in the inner 160 kpc from 1/4 of the solar value to the solar value without difficulty. In fact, the starburst is considerably more compact than the metal-enhanced central region of the cluster. Were the metals produced by the starburst confined to the star formation region, the hot gas would become enriched to levels well above the solar value, which is not observed. This problem might be circumvented if the metal-rich gas produced by the burst has been transported outward and mixed with the lower metallicity gas in the halo by a merger or an outflow driven by the AGN. Alternatively, the metals produced in the starburst may be primarily locked in the cold gas and are unable to enhance the metallicity of the hot gas. Finally, the observed metallicity gradient could have been imprinted by stellar evolution of the cD galaxy's older population (De Grandi et al. 2004). This issue will be explored further in a future paper.

3.5. *Comparison Between the Cooling Rate and Star Formation Rate*

The starburst in Abell 1835 sits in a region where the cooling time has fallen below 6×10^8 yr, which is close to the age of the starburst. The temperature of the gas has also reached a minimum of 3.5 keV there, which is similar to other cooling flow systems, such as Hydra A (McNamara et al. 2000) and Abell 1068 (McNamara et al. 2004). These conditions are qualitatively consistent with expectations for fueling by the cooling flow. However, quantitative consistency requires that there be mass continuity between the rate of cooling and its sink. The vast gulf between radiative cooling rates and star formation has cast a pall on the pure (no feedback) cooling flow model since it was conceived nearly 30 yr ago.

An observation made with *XMM-Newton*'s reflection grating spectrometer (Peterson et al. 2003) shows that the gas in Abell 1835 is cooling at a rate of between 1000–2000 $M_\odot$ yr^{-1} from the mean gas temperature of nearly 9 keV to about 2 keV, where cooling slows dramatically (Peterson et al. 2003). Below 2 keV, cooling proceeds at a much reduced rate of $\lesssim$200 $M_\odot$ yr^{-1}. Whether any cooling out of the X-ray band occurs is still to be demonstrated. However, cooling at this reduced rate is now consistent with the star formation rate in the cD galaxy. Provided there is an active heating mechanism to offset the remaining cooling luminosity, which we justify below, the (reduced) cooling model is now consistent with a sink in star formation and the central black hole. This situation is evidently true in an increasing fraction of cooling flow clusters (Rafferty et al. 2006).

4. FEEDBACK AND REGULATED COOLING IN THE CLUSTER'S CORE

The data discussed in § 3 are consistent with an active but relatively moderate cooling flow. Nevertheless, the gas throughout the central 150 kpc of the cluster has a cooling time that is shorter than the cluster's age (Fig. 7), yet most of this gas is not condensing out. The radiation losses from this gas,

$$L_{cool} \simeq 1.2 \times 10^{45} \left(\frac{\dot{M}}{1000\ M_\odot\ \mathrm{yr}^{-1}} \right) \mathrm{ergs\ s}^{-1}, \qquad (1)$$

must then be replenished by heating (Fabian et al. 2001; Böhringer et al. 2002). We now consider whether thermal conduction, the AGN, and supernova explosions are able to compensate the radiative losses.

4.1. *Feedback from the Starburst*

Here, we adopt an optimistic star formation rate of 180 $M_\odot$ yr^{-1}, and we follow closely the discussions in McNamara et al. (2004) and Wise et al. (2004). We assume a blast energy per Type II supernova of 10^{51} ergs and a Type II supernova production rate of 1 per 127 $M_\odot$ of star formation (Hernquist & Springel 2003). These values then yield an average energy injection rate over

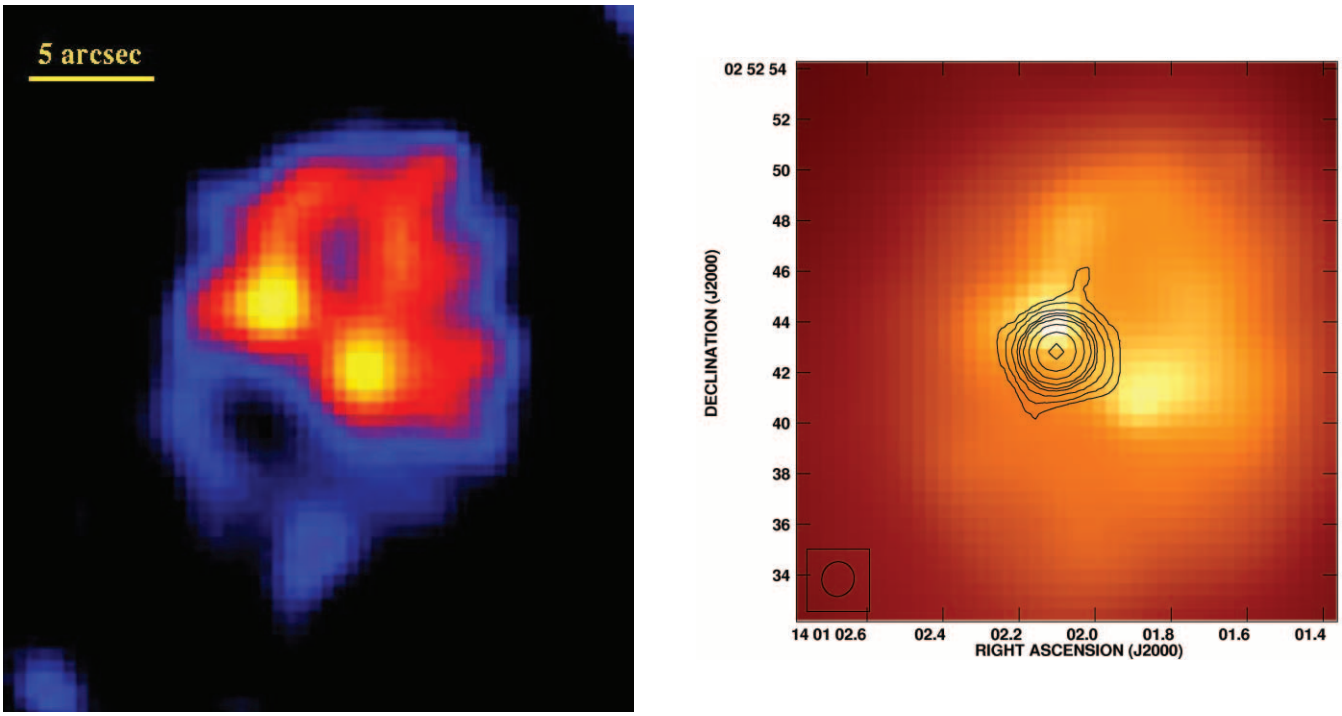

FIG. 9.—*Left*: 66.5 ks image of the core of the cluster taken recently with the ACIS-I detector (M. W. Wise et al. 2006, private communication) showing the pair of cavities to the northwest and southeast of the nucleus, which lies between the bright spots of emission near the center of the picture. *Right*: Shorter ACIS-S X-ray image on which the X-ray analysis was done showing the radio source superposed.

the life of the starburst of 4.5×10^{43} ergs s^{-1}. This is at most a few percent of the power required to quench the cooling flow, even with efficient coupling between the supernova blast energy and the hot gas. This figure can be boosted by adopting an extreme supernova yield per mass or an IMF richer in massive stars than the Salpeter function. However, the requirements are still extreme in view of earlier arguments weighing against an IMF that is dramatically different from Salpeter's. Supernovae may be an important source of heat in the region surrounding the starburst and AGN, but they cannot have a substantial effect on the overall cooling flow. The same conclusion was reached for the Abell 1068 cluster cD galaxy (McNamara et al. 2004). Since both are among the most massive starbursts known in cooling flows, this conclusion probably holds in most systems.

4.2. *Heating by Thermal Conduction*

The conditions in which inward-flowing heat from the hot layers of gas surrounding the cooling core are able to replenish radiation losses have been studied extensively in recent years (Fabian et al. 2002; Zakamska & Narayan 2003; Voigt & Fabian 2004). Abell 1835 has been examined in this context but with contradictory results. Zakamska & Narayan (2003) were apparently able to construct theoretical gas temperature, density, and cooling profiles that matched those of Abell 1835 using an inward heat flux proceeding at 40% of the *Spitzer* rate. On the other hand, Voigt & Fabian (2004) found that heat conduction proceeding at a modest fraction of the *Spitzer* rate could quench cooling only in the outer reaches of the cooling region but not near the central starburst, where the gas temperature is rapidly decreasing. In order to balance radiative losses, they found that the conductivity must exceed the *Spitzer* value within the radius at which the gas falls below 7 keV. The conductivity reaches 1/3 of the *Spitzer* value where the gas temperature is approximately 10 keV. The corresponding radii are 20″ (79 kpc) and 40″ (157 kpc), respectively. It seems reasonable then to expect thermal conduction to balance radiation losses in the outer parts of the cooling region, but to be unable to do so in the central region near the starburst. Although similar conclusions were reached for the Abell 1068 cluster (Wise et al. 2004), the importance of conduction without knowledge of the conductivity of the gas is difficult to evaluate with confidence.

4.3. *AGN Feedback: X-Ray Cavities*

The structure in the inner 10″ of the X-ray image shown in Figure 9 was first reported by Schmidt et al. (2001), who attributed it, we now believe incorrectly, to a recent merger. Two surface brightness depressions with count deficits of approximately 20%–40% compared to the surrounding emission are seen in the ACIS-S images 6″ (23 kpc) to the northwest and 5″ (17 kpc) to the southeast of the cD's nucleus. The cavities were confirmed by the 66.5 ks ACIS-I image shown at left in Figure 9. The nucleus lies in the trough between the two bright central knots of emission. The trough might be caused by photoelectric absorption of X-rays by the molecular gas clouds. The cavities have bright rims and otherwise resemble the AGN-induced X-ray cavities now seen in more than two dozen clusters (Rafferty et al. 2006; Bîrzan et al. 2004; Dunn & Fabian 2004). Their physical characteristics are given in Table 2, including their distances from the nucleus, the sizes of their major and minor axes, the surrounding gas pressures and deprojected temperatures, the pV energies of the cavities, and the approximate buoyancy ages (see Bîrzan et al. 2004).

We were initially concerned that the cavities themselves might be caused by photoelectric absorption from the molecular gas in the cD. Edge & Frayer (2003) found a column density of 4×10^{22} cm^{-2} in the inner 10 kpc region of the cD galaxy, which is centrally concentrated and does not correspond to the two off-axis surface brightness depressions. We found a small excess

TABLE 2
CAVITY PROPERTIES

Cavity	R (kpc)	a (kpc)	b (kpc)	p (10^{-9} ergs cm^{-3})	kT (keV)	pV (10^{59} ergs)	t (Myr)
Northwest.....	23.3	15.5	11.6	1.0 ± 0.1	4.3 ± 0.4	$2.6^{+2.9}_{-1.0}$	41
Southeast.....	16.6	13.6	9.7	1.1 ± 0.1	3.8 ± 0.3	$1.7^{+1.8}_{-0.3}$	27

column density of $\sim 3 \times 10^{21}$ cm^{-2} from the X-ray spectrum of the inner 10″ or so, as do Schmidt et al. (2001), which could be the diluted column of molecular gas. However, because the cavities are seen in both hard and soft images above and below 2 keV, they cannot be due to photoelectric absorption, which dominates below 2 keV.

The sizes of the cavities are more or less typical of those found in massive clusters (e.g., Bîrzan et al. 2004; Dunn & Fabian 2004). However, the central pressure of 1.1×10^{-9} ergs cm^{-3} is more than an order of magnitude larger than is typically found at the base of a cooling flow. The work required to inflate the cavities against the surrounding pressure is $pV = 4.3^{+4.6}_{-1.5} \times 10^{59}$ ergs. This corresponds to a mean mechanical power of $L = 3.5^{+3.0}_{-1} \times 10^{44}$ ergs s^{-1}, assuming a rise time of about 40 Myr. The total enthalpy is roughly 2.5–4 times larger, depending on the equation of state of the gas filling the cavity (Bîrzan et al. 2004). This implies a total jet power of $\sim 1.4 \times 10^{45}$ ergs s^{-1}, which is comparable to the cooling luminosity of a 1000–2000 $M_\odot$ yr^{-1} cooling flow. So long as the coupling between the AGN and the gas is reasonably efficient, the AGN power is high enough to offset radiation losses in this system.

The cD galaxy harbors a compact radio source shown in Figure 9. The image obtained from the Very Large Array archive was taken in the A configuration at a frequency of 1.4 GHz. The resolution of the image is about 1″. The spectral index $\alpha = 0.65$ ($f_\nu \propto \nu^{-\alpha}$) implies a total radio luminosity of $(3.55 \pm 0.09) \times 10^{41}$ ergs s^{-1} between 10 MHz and 10 GHz. (A more complete discussion of the radio properties will be given in a forthcoming paper.) The radio source at this frequency shows no obvious connection to the cavity system; however, the 330 MHz map (also discussed in a forthcoming paper) covers the entire extent of the cavities, but again shows no detailed correlation with the holes. The low-frequency source is probably the remnant synchrotron emission from the outburst that occurred about 40 Myr ago.

The nucleus of Abell 1835 is a striking example of how poorly radio synchrotron emission traces true jet power. The average jet power required to inflate the cavities, $\sim 1.4 \times 10^{45}$ ergs s^{-1}, dwarfs the total radio synchrotron power, exceeding it by a factor of 4000. The corresponding synchrotron radiative efficiency is then only about 0.02%, which is vastly smaller than $\sim$1% found for M87 (Owen et al. 2000) and other sources (De Young 1993; Bicknell et al. 1997).

5. SIMULTANEOUS GROWTH OF THE BULGE AND THE SUPERMASSIVE BLACK HOLE

The magnitude of the AGN outburst implies that the central black hole has accreted $\simeq 4pV/\epsilon c^2 = 1.1 \times 10^7\ M_\odot$ ($\epsilon = 0.1$) in the past 40 Myr or so, corresponding to an average accretion rate of $\sim 0.3\ M_\odot$ yr^{-1} (Rafferty et al. 2006). Adopting the star formation rate as an estimate of the current bulge growth rate (see Rafferty et al. [2006] for a more detailed discussion), we find that the bulge has added between 300 and 600 units of mass for every 1 unit that has fallen into the black hole. This relative growth rate is intriguingly close to the slope of the Magorrian relation between bulge and black hole mass in quiescent galaxies (Häring & Rix 2004). The convergence of several factors, including the fact that star formation in the cD is proceeding at a rate that rivals or exceeds those observed during the peak years of galaxy formation (Juneau et al. 2005), suggests that the physical conditions driving this growth could be analogous to those that held in the early universe when the Magorrian relation was presumably imprinted on galaxies. The cooling flow systems probably differ, however, in that their accretion is substantially sub-Eddington. The conditions in Abell 1835 should be placed in context with similar systems, which clearly show a trend between star formation and black hole growth, but there is a great deal of scatter (Rafferty et al. 2006). In some systems the black hole has grown by a substantial fraction of its mass in a single outburst but with little commensurate bulge growth over the same time period (McNamara et al. 2005; Nulsen et al. 2005a). In other systems, such as Abell 1068 (McNamara et al. 2004), the bulge is growing much faster than the black hole. In general, cooling flow cD galaxies and their black holes have evidently not grown in lock-step over the past several billion years (Rafferty et al. 2006).

6. SUMMARY AND DISCUSSION

The cD galaxy in Abell 1835 is in the midst of a starburst proceeding at a rate of 100–180 $M_\odot$ yr^{-1} that began approximately 320 Myr ago. The star formation rate is consistent with the maximum rate that gas can be condensing out of the cooling flow. Cooling and accretion at this level can account for only 10%–20% of the total radiative losses, implying that the bulk of the gas is being heated and maintained at X-ray temperatures. Supernovae in the starburst are energetically incapable of producing enough heat to do so, and thermal conduction is ineffective in the inner regions of the cooling flow.

We discovered a pair of cavities in the hot gas produced by a powerful AGN outburst that occurred roughly 40 Myr ago. The outburst was energetic enough to offset the remaining radiative losses. There is no longer a discrepancy between the radiative cooling rate and the sink of the cooling gas, provided the jet power heats the gas efficiently. The jet power required to produce the cavities exceeds the radio synchrotron power by $\simeq$4000 times, indicating a radiatively inefficient yet powerful radio source.

The jet power 1.4×10^{45} ergs s^{-1} corresponds to the Eddington luminosity of a $\sim 10^7\ M_\odot$ black hole. However, the K-band luminosity of the host cD galaxy implies a much larger black hole mass of approximately $5 \times 10^9\ M_\odot$ (Rafferty et al. 2006), implying that accretion is proceeding at a small fraction $\sim 3 \times 10^{-3}$ of the Eddington rate. This exceeds the Bondi rate by nearly 500 times, assuming the measured central gas density holds near the unresolved Bondi radius (Rafferty et al. 2006). Minding the uncertain assumptions about the black hole mass and surrounding gas density, Bondi accretion could contribute at some level, but is unlikely to be primarily responsible for feeding the outburst. The large pool of centrally condensed molecular gas is consistent with cold accretion. If the molecular gas is fed by gas condensing out of the hot phase, it would provide a natural supply of fuel necessary to maintain an AGN feedback loop. We

cannot, however, exclude the possibility that the gas arrived through a merger.

The rate of black hole growth implied by the jet power and bulge growth through star formation are consistent with the slope of the (Magorrian) relationship between bulge mass and black hole mass for quiescent bulges. This surprising result suggests that feedback processes like those operating in this system could be driving the relationship between bulge mass and supermassive black hole mass in normal bulges (Magorrian et al. 1998; Kormendy & Richstone 1995; Springel et al. 2005). In a large sample of cooling flows, Rafferty et al. (2006) have found a trend between bulge growth rate through star formation and black hole growth rate over the past $\sim$1 Gyr. However, the large scatter in the relative rates implies that bulge and black hole growth do not always proceed in lockstep. This result also supports the growing consensus that AGN feedback could explain the exponential decline in luminous galaxies relative to the predicted shape of the dark matter halo mass function by suppressing cooling (Benson et al. 2003; Croton et al. 2006; Best et al. 2006). Consequently, the mode of accretion in this and other cooling flow systems should hold considerable interest to more general models of galaxy formation (e.g., Croton et al. 2006; Soker 2006; Pizzolato & Soker 2005; Sijacki & Springel 2006).

Abell 1835's nuclear outburst is as powerful as a quasar's, and its starburst is proceeding at a rate that rivals those in burgeoning galaxies beyond $z = 2$. However, there are noteworthy differences in the way the gravitational binding energy of accretion is channeled away from the black hole. While quasars radiate away most of their accretion energy, the accretion energy emerging from Abell 1835 and other cooling flows is almost entirely mechanical. Abell 1835's jet power, $\sim 1.4 \times 10^{45}$ ergs s^{-1}, exceeds postulated protogalactic wind luminosities (Silk & Rees 1998) by an order of magnitude, as it must to all but stop the cooling flow. However, strong nonthermal nuclear emission and broad emission lines are absent, and the radiative efficiency of the radio source, defined as the ratio of radio synchrotron power to jet power, is very low. This may be a characteristic of the late stages of galaxy formation, when accretion onto the black hole falls below the Eddington rate, which probably held during the early stages of galaxy formation (Silk & Rees 1998; Blandford 1999; Begelman & Nath 2005; Churazov et al. 2005). Even so, long-lived accretion at the present rate would continue to drive star formation and black hole growth such that the relationship between bulge and black hole mass found in quiescent elliptical galaxies would be imprinted or maintained.

Following a checkered and often contentious history, the cooling flow problem is now coming to resolution. We should emphasize, however, that the model must still pass an essential test. Gas cooling out of the intracluster medium should emit detectable X-ray cooling lines, notably the Fe XVII line at 15 Å (0.826 keV). In this case, the flux scales as

$$f(\mathrm{Fe\ XVII}) = 5.456 \times 10^{-15} \left(\frac{\dot{M}}{100\ M_{\odot}\ \mathrm{yr}^{-1}} \right) \times \left(\frac{D}{500\ \mathrm{Mpc}} \right)^{-2} \mathrm{ergs\ s^{-1}\ cm^{-2}}, \quad (2)$$

where D is the distance and $\dot{M}$ is the cooling rate. Peterson et al.'s (2003) limits successfully ruled-out wholesale cooling, but they generally lie well above the levels of accretion implied by the observed star formation rates (Rafferty et al. 2006). A cooling rate $\dot{M}$ approximately equal to the observed star formation rates is currently detectable using deep *XMM-Newton* observations and will be using shorter observations with the *Constellation-X* observatory in the future. For the half dozen or so objects whose star formation rates are comparable to the available cooling upper limits (including Abell 1835 and Abell 1068), a 200–400 ks *XMM-Newton* observation using the reflection grating spectrometer would be sufficient to restrictively test the cooling flow/feedback model of galaxy formation.

This research was funded by NASA Long Term Space Astrophysics grant NAG 4-11025.

REFERENCES

Allen, S. W. 1995, MNRAS, 276, 947
Arnaud, K. A. 1996, in ASP Conf. Ser. 101, Astronomical Data Analysis Software and Systems V, ed. G. H. Jacoby & J. Barnes (San Francisco: ASP), 17
Balogh, M. L., Pearce, F. R., Bower, R. G., & Kay, S. T. 2001, MNRAS, 326, 1228
Basson, J. F., & Alexander, P. 2003, MNRAS, 339, 353
Begelman, M. C., & Nath, B. B. 2005, MNRAS, 361, 1387
Benson, A. J., Bower, R. G., Frenk, C. S., Lacey, C. G., Baugh, C. M., & Cole, S. 2003, ApJ, 599, 38
Bertschinger, E., & Meiksin, A. 1986, ApJ, 306, L1
Best, P. N., et al. 2006, MNRAS, 368, L67
Bicknell, G. V., Dopita, M. A., & O'Dea, C. P. O. 1997, ApJ, 485, 112
Binney, J. 2004, Phil. Trans. R. Soc. London A, 363, 739
Bîrzan, L., Rafferty, D. A., McNamara, B. R., Wise, M. W., & Nulsen, P. E. J. 2004, ApJ, 607, 800
Blanchard, A., Valls-Gabaud, D., & Mamon, G. A. 1992, A&A, 264, 365
Blandford, R. D. 1999, preprint (astro-ph/9906025)
Blanton, E. L., Sarazin, C. L., & McNamara, B. R. 2003, ApJ, 585, 227
Böhringer, H., & Hensler, G. 1989, A&A, 215, 147
Böhringer, H., Matsushita, K., Churazov, E., Ikebe, Y., & Chen, Y. 2002, A&A, 382, 804
Borgani, S., Governato, F., Wadsley, J., Menci, N., Tozzi, P., Quinn, T., Stadel, J., & Lake, G. 2002, MNRAS, 336, 409
Brighenti, F., & Mathews, W. G. 2002, ApJ, 573, 542
Brüggen, M. 2003, ApJ, 592, 839
Brüggen, M., & Kaiser, C. R. 2001, MNRAS, 325, 676
———. 2002, Nature, 418, 301
Bruzual, G., & Charlot, S. 2003, MNRAS, 344, 1000
Burns, J. O. 1990, AJ, 99, 14
Cardelli, J. A., Clayton, G. C., & Mathis, J. S. 1989, ApJ, 345, 245
Churazov, E., Brüggen, M., Kaiser, C. R., Böhringer, H., & Forman, W. 2001, ApJ, 554, 261
Churazov, E., Sazonov, S., Sunyaev, R., Forman, W., Jones, C., & Böhringer, H. 2005, MNRAS, 363, L91
Churazov, E., Sunyaev, R., Forman, W., Böhringer, H. 2002, MNRAS, 332, 729
Ciotti, L., & Ostriker, J. P. 1997, ApJ, 487, L105
Cole, S. 1991, ApJ, 367, 45
Coleman, G. D., Wu, C.-C., & Weedman, D. W. 1980, ApJS, 43, 393
Cowie, L. L., & Binney, J. 1977, ApJ, 215, 723
Crawford, C. S., Allen, S. W., Ebeling, H., Edge, A. C., & Fabian, A. C. 1999, MNRAS, 306, 857
Crawford, C. S., Sanders, J. S., & Fabian, A. C. 2005, MNRAS, 361, 17
Croton, D. J., et al. 2006, MNRAS, 365, 11
David, L. P., Nulsen, P. E. J., McNamara, B. R., Forman, W., Jones, C., Ponman, T., Robertson, B., & Wise, M. 2001, ApJ, 557, 546
De Grandi, S., Ettori, S., Longhetti, M., & Molendi, S. 2004, A&A, 419, 7
De Young, D. S. 1993, ApJ, 402, 95
———. 2003, MNRAS, 343, 719
Dickey, J. M., & Lockman, F. J. 1990, ARA&A, 28, 215
Donahue, M., Mack, J., Voit, G. M., Sparks, W., Elston, R., & Maloney, P. R. 2000, ApJ, 545, 670
Donahue, M., Horner, D. J., Cavagnolo, K. W., & Voit, G. M. 2006, ApJ, 643, 730
Dunn, R. J. H., & Fabian, A. C. 2004, MNRAS, 355, 862
Edge, A. C. 2001, MNRAS, 328, 762
Edge, A. C., & Frayer, D. T. 2003, ApJ, 594, L13

Fabian, A. C. 1994, ARA&A, 32, 277
Fabian, A. C., Mushotzky, R. F., Nulsen, P. E. J., & Peterson, J. R. 2001, MNRAS, 321, L20
Fabian, A. C., & Nulsen, P. E. J. 1977, MNRAS, 180, 479
Fabian, A. C., Sanders, J. S., Crawford, C. S., Conselice, C. J., Gallagher, J. S., & Wyse, R. F. G. 2003, MNRAS, 344, L48
Fabian, A. C., Voigt, L. M., & Morris, R. G. 2002, MNRAS, 335, L71
Falcke, H., Rieke, M. J., Rieke, G. H., Simpson, C., & Wilson, A. S. 1998, ApJ, 494, L155
Ferrarese, L., & Merritt, D. 2000, ApJ, 539, L9
Finoguenov, A., & Jones, C. 2001, ApJ, 547, L107
Forman, W., et al. 2005, ApJ, 635, 894
Gallagher, J. S., & Ostriker, J. P. 1972, AJ, 77, 288
Gebhardt, K., et al. 2000, ApJ, 539, L13
Gómez, P. L., Loken, C., Roettiger, K., & Burns, J. O. 2002, ApJ, 569, 122
Häring, N., & Rix, H. W. 2004, ApJ, 604, L89
Hausman, M. A., & Ostriker, J. P. 1978, ApJ, 224, 320
Heckman, T. M., Baum, S. A., van Breugel, W. J. M., & McCarthy, P. 1989, ApJ, 338, 48
Heinz, S., Choi, Y.-Y., Reynolds, C. S., & Begelman, M. C. 2002, ApJ, 569, L79
Hernquist, L., & Springel, V. 2003, MNRAS, 341, 1253
Hicks, A. K., & Mushotzky, R. 2005, ApJ, 635, L9
Jaffe, W. 1990, A&A, 240, 254
Jaffe, W., Bremer, M. N., & Baker, K. 2005, MNRAS, 360, 748
Jaffe, W., Bremer, M. N., & van der Werf, P. P. 2001, MNRAS, 324, 443
Jia, S. M., Chen, Y., Lu, F. J., & Xiang, F. 2004, A&A, 423, 65
Johnstone, R. M., Fabian, A. C., & Nulsen, P. E. J. 1987, MNRAS, 224, 75
Jones, T. W., & De Young, D. S. 2005, ApJ, 624, 586
Juneau, J., et al. 2005, ApJ, 619, L135
Kaiser, C. R., & Binney, J. 2003, MNRAS, 338, 837
Kauffmann, G. 1996, MNRAS, 281, 475
Kennicutt, R. C. 1998, ApJ, 498, 541
Kormendy, J., & Richstone, D. 1995, ARA&A, 33, 581
Kraft, R. P., et al. 2006, ApJ. 639, 753
Magorrian, J., et al. 1998, AJ, 115, 2285
Majerowicz, S., Neumann, D. M., & Reiprich, T. H. 2002, A&A, 394, 77
Markevitch, M. 2002, preprint (astro-ph/0205333)
McNamara, B. R. 2004, in The Riddle of Cooling Flows in Galaxies and Clusters of Galaxies, ed. T. H. Reiprich, J. C. Kempner, & N. Soker (Charlottesville: Univ. Virginia), http://www.astro.virginia.edu/coolflow/
McNamara, B. R., Nulsen, P. E. J., Wise, M. W., Rafferty, D. A., Carilli, C., Sarazin, C. L., & Blanton, E. L. 2005, Nature, 433, 45
McNamara, B. R., & O'Connell, R. W. 1989, AJ, 98, 2018
———. 1992, ApJ, 393, 579
———. 1993, AJ, 105, 417
McNamara, B. R., O'Connell, R. W., & Bregman, J. N. 1990, ApJ, 360, 20
McNamara, B. R., Wise, M. W., & Murray, S. S. 2004, ApJ, 601, 173
McNamara, B. R., et al. 2000, ApJ, 534, L135
———. 2001, ApJ, 562, L149
Merritt, D. 1985, ApJ, 289, 18
Metzler, C. A., & Evrard, A. E. 1994, ApJ, 437, 564
Molendi, S., & Pizzolato, F. 2001, ApJ, 560, 194
Narayan, R., & Medvedev, M. V. 2001, ApJ, 562, L129
Nulsen, P. E. J., David, L. P., McNamara, B. R., Jones, C., Forman, W. R., & Wise, M. 2002, ApJ, 568, 163
Nulsen, P. E. J., Hambrick, D. C., McNamara, B. R., Rafferty, D., Birzan, L., Wise, M. W., & David, L. P. 2005a, ApJ, 625, L9
Nulsen, P. E. J., McNamara, B. R., Wise, M. W., & David, L. P. 2005b, ApJ, 628, 629
O'Dea, C. P., Baum, S. A., & Gallimore, J. F. 1994, ApJ, 436, 669
Omma, H., Binney, J., Bryan, G., & Slyz, A. 2004, MNRAS, 348, 1105
Owen, F. N., Eilek, J. A., & Kassim, N. E. 2000, ApJ, 543, 611
Peletier, R. F., Davies, R. L., Illingworth, G. D., Davis, L. E., & Cawson, M. 1990, AJ, 100, 1091
Peterson, J. R., Kahn, S. M., Paerels, F. B., Kaastra, J. S., Tamura, T., Bleeker, J. A. M., Ferrigno, C., & Jernigan, J. G. 2003, ApJ, 590, 207
Peterson, J. R., et al. 2001, A&A, 365, L104
Piffaretti, R., & Kaastra, J. S. 2006, A&A, 453, 423
Pizzolato, F., & Soker, N. 2005, ApJ, 632, 821
Porter, A. C., Schneider, D. P., & Hoessel, J. G. 1991, AJ, 101, 1561
Quilis, V., Bower, R. G., & Balogh, M. L. 2001, MNRAS, 328, 1091
Rafferty, D. A., McNamara, B. R., Nulsen, P. E. J., & Wise, M. W. 2006, ApJ, in press
Reynolds, C. S., Heinz, S., & Begelman, M. C. 2002, MNRAS, 332, 271
Rosner, R., & Tucker, W. H. 1989, ApJ, 338, 761
Ruszkowski, M., & Begelman, M. C. 2002, ApJ, 581, 223
Ruszkowski, M., Brüggen, & Begelman, M. 2004, ApJ, 615, 675
Salomé, P., & Combes, F. 2003, A&A, 412, 657
Sarazin, C. L. 1986, Rev. Mod. Phys., 58, 1
Sarazin, C. L., & O'Connell, R. W. O. 1983, ApJ, 268, 552
Schmidt, M. 1959, ApJ, 129, 243
Schmidt, R. W., Allen, S. W., & Fabian, A. C. 2001, MNRAS, 327, 1057
Schombert, J. M. 1986, ApJS, 60, 603
Sijacki, D., & Springel, V. 2006, MNRAS, 366, 397
Silk, J., Djorgovski, S., Wyse, R. F. G., & Bruzual, A., G. 1986, ApJ, 307, 415
Silk, J., & Rees, M. 1998, A&A, 331, L1
Soker, N. 2006, NewA, in press (astro-ph/0602043)
Soker, N., Blanton, E. L., & Sarazin, C. L. 2002, ApJ, 573, 533
Soker, N., White, R. E., David, L. P., & McNamara, B. R. 2001, ApJ, 549, 832
Springel, V., Di Matteo, T., & Hernquist, L. 2005, MNRAS, 361, 776
Tabor, G., & Binney, J. 1993, MNRAS, 263, 323
Tamura, T., et al. 2001, A&A, 365, L87
Taylor, G. B. 1996, ApJ, 470, 394
Tucker, W. H., & Rosner, R. 1983, ApJ, 267, 547
Vernaleo, J. C., & Reynolds, C. S. 2005, preprint (astro-ph/0511501)
Voigt, L. M., & Fabian, A. C. 2004, MNRAS, 347, 1130
Voigt, L. M., Schmidt, R. W., Fabian, A. C., Allen, S. W., & Johnstone, R. M. 2002, MNRAS, 335, L7
Voit, G. M. 2005, Rev. Mod. Phys.,77, 207
Voit, G. M., & Donahue, M. 1997, ApJ, 486, 242
———. 2005, ApJ, 634, 955
White, S. D. M., & Rees, M. J. 1978, MNRAS, 183, 341
Wise, M. W., McNamara, B. R., & Murray, S. S. 2004, ApJ, 601, 184
Wu, K. K. S., Fabian, A. C., & Nulsen, P. E. J. 2000, MNRAS, 318, 889
Young, A. J., Wilson, A. S., & Mundell, C. G. 2002, ApJ, 579, 560
Zakamska, N. L., & Narayan, R. 2003, ApJ, 582, 162